Journal of The Electrochemical Society, **154** (10) F177-F185 (2007)
0013-4651/2007/154(10)/F177/9/$20.00 © The Electrochemical Society

Simulation of Wet-Dry Cycling of Organic Coatings Using Ionic Liquids

K. N. Allahar,[a,*,z] B. R. Hinderliter,[a] A. M. Simoes,[b,*] D. E. Tallman,[a,c,*] G. P. Bierwagen,[a,*] and S. G. Croll[a]

[a]*Department of Coatings and Polymeric Materials, and* [c]*Department of Chemistry and Molecular Biology, North Dakota State University, Fargo, North Dakota 58105, USA*
[b]*ICMES/Chemical Engineering Department, Instituto Superior Tecnico, Lisboa, Portugal*

The capacitance evolution of an organic coating undergoing cyclic wetting and drying conditions was monitored by single frequency electrochemical impedance spectroscopy. Monitoring of the drying condition was possible with the use of a hydrophilic room temperature ionic liquid and the methodology employed is presented. Experimental results associated with cyclic dilute NaCl wetting and ionic liquid drying are presented for an epoxy coating on an AA 2024-T3 substrate. The calculated capacitance evolutions associated with wetting and drying were generally consistent with Fick's second law. The calculation of the water ingress and egress diffusion coefficients using a short-time approximate solution and a series solution to Fick's second law are presented. The latter solution is shown to address the capacitance evolution better than the former with the ingress coefficient larger than the egress coefficient for a given exposed coating surface. There was agreement between the calculated diffusion coefficient ingress values for coating areas exposed to cyclic NaCl wetting—ionic liquid drying and cyclic NaCl wetting—natural drying conditions. Comparison of the impedance spectra for test areas indicated that the use of the ionic liquid as a drying medium influenced the electrochemical properties of the coating only after a number of cycles.
 [DOI: 10.1149/1.2764235]

Manuscript submitted October 19, 2006; revised manuscript received June 1, 2007. Available electronically August 7, 2007.

The protection of metallic structures by organic coatings is primarily due to the isolation of the structure from the environment by the coating. The barrier protection provided by a coating is influenced by the absorption of water and ionic species from the environment. Literature associated with the measurement of water absorption of a polymer film has been reported using gravimetry.[1-7] A parameter that significantly influences the transport properties of a coating is the diffusion coefficient of water into the coating D_{in}. An idealized model that relates the mass changes associated with absorption to D_{in} for an organic coating is based on the series solution of Fick's second law.[3,4,8] An approximation to the series solution that is applicable for short times is employed in literature to calculate D_{in} based on gravimetric measurements.[3,5,6] The series solution to Fick's second law and the approximate solutions are also applicable to mass changes associated with desorption of water.

The different dielectric properties of water and an organic coating result in changes in the capacitance of the coating that accompanies water absorption or desorption.[1,2] The monitoring of the capacitance by electrochemical impedance spectroscopy (EIS) has provided a convenient method for the volumetric evaluation of water absorption in organic coatings.[3,4,7,9-15] The capacitance evolution of an organic coating can be used to calculate D_{in} by relating the volumetric changes associated with water absorption with the mass changes.[3,4,11,14,15]

Metallic structures covered with a protective organic coating exposed to outdoor conditions are subjected to cyclic wetting and drying conditions. The measurements of the water absorption and desorption for a coating under cyclic wet-dry conditions by gravimetry[2] and capacitance changes have been reported.[13] In these reports the wetting stage involved immersion in an aqueous electrolyte and the drying stage involved exposure to air. Recently an experimental setup has been reported where the drying stage of a wet-dry cycle was simulated using a hydrophilic room temperature ionic liquid (RTIL).[14] The single frequency impedance responses associated with the wetting and drying stages were used to calculate the capacitance evolution for the cycles. The capacitance data were used to calculate the diffusion coefficient values associated with the wetting D_{in} and drying D_{out} stages.

RTILs are salts that have melting points close to or below room temperature. They are chemically stable and have extremely low vapor pressures and low toxicity. Their ionic conductivities are over 0.01 Scm^{-1} at room temperature.[16] The conduction afforded by the ionic liquid permitted a nonaqueous medium for electrochemical measurements. There has been increasing use of RTILs for analytical chemistry and electrochemistry, and electrochemical applications have been reported that were associated with the corrosion of metals, electrodeposition of metals and semiconductors, supercapacitor electrolyte, and for non-Li battery.[17,18]

Results associated with an experimental procedure employing cyclic 0.05 M NaCl wetting and RTIL drying conducted on samples of epoxy coating on AA 2024-T3 are presented and discussed. A control experiment was also conducted where a natural drying stage was used, by exposure to air in a dessicator, instead of the RTIL drying stage. The capacitance data obtained from these experiments were analyzed using models to determine the values of D_{in} and D_{out}. Experiments were also conducted where EIS spectra were obtained for the samples under constant immersion in 0.05 M NaCl and RTIL. The data from these experiments were used to compare wet-dry cycling with constant immersion, and to determine whether the use of RTILs was suitable for simulating drying conditions.

The use of RTILs as a medium to monitor the drying process of an organic coating is novel. However, a limitation to the approach is the influence of the RTIL on the electrochemical properties of the coating. Results are presented that demonstrate that the RTIL did not influence the coating properties under constant immersion but only after several NaCl wet-RTIL dry cycles. This may be addressed by using a RTIL with larger ions such that entry into the coating by diffusion or through pores would be reduced.

An idealized model for the diffusion of water into an organic coating is based on the solution of the Fick's second law

$$\frac{\partial c(z,t)}{\partial t} = D\frac{\partial^2 c(z,t)}{\partial z^2} \qquad [1]$$

where c and D are the concentration and diffusion coefficient of water, respectively.[3] The independent variables are the position z, measured from a reference point, and the time t. A form of the solution is given as

$$\frac{M_t}{M_s} = 1 - \frac{8}{\pi^2}\sum_{n=0}^{\infty}\frac{1}{(2n+1)^2}\exp\left(\frac{-(2n+1)^2 D\pi^2}{4L^2}t\right) \qquad [2]$$

where M_t and M_s represent the mass of water absorbed at time t and at saturation, respectively, and L is the coating thickness.[2,8] This solution is based on the assumption that D is independent of c. The

* Electrochemical Society Active Member.
z E-mail: Kerry.Allahar@ndsu.edu

solution is applicable to a system absorbing water as well as desorbing water, and, as such D can be either D_{in} or D_{out}.[8] The term on the left-hand side of Eq. 2 represents the degree of saturation of the coating. An approximate solution[15] for Eq. 2 applicable for short times involves replacing the summation by an integration to yield

$$\frac{M_t}{M_s} = \sqrt{\frac{4Dt}{L^2\pi}} \quad [3]$$

The volume fraction that is occupied by water ϕ_t at a time t is given by

$$\phi_t = \frac{\log(C_t/C_0)}{\log \varepsilon_{H_2O}} \quad [4]$$

where C_0 and C_t represent the coating capacitance at $t = 0$ and at any time t, respectively, and ε_{H_2O} represents the permittivity of water.[1] The degree of saturation of the coating expressed by the ratio of volume fraction at time t to that at saturation ϕ_s is given by

$$\frac{\phi_t}{\phi_s} = \frac{\log(C_t/C_0)}{\log(C_s/C_0)} \quad [5]$$

where C_s represent the coating capacitance at saturation.[1,2]

Combinations of Eq. 2 and 5

$$\frac{\log(C_t/C_0)}{\log(C_s/C_0)} = 1 - \frac{8}{\pi^2}\sum_{n=0}^{\infty}\frac{1}{(2n+1)^2}\exp\left(\frac{-(2n+1)^2 D\pi^2}{4L^2}t\right) \quad [6]$$

and Eq. 3 and 5

$$\frac{\log(C_t/C_0)}{\log(C_s/C_0)} = \sqrt{\frac{4Dt}{L^2\pi}} \quad [7]$$

yield two ways of calculating the value of D from capacitance measurements based on either the series solution or a short-time approximation, respectively. These ways would be referred to as the series model and the short-time model, respectively.

Experimental

The coating system used in the experiments consisted of a one-layer, nonpigmented epoxy on an AA 2024-T3 substrate. The mill finished AA 2024-T3 panels, supplied by Q-Panel Lab Products of Cleveland, OH, were washed in deionized water and cleaned with hexane before application of the epoxy. The two-component epoxy was made by mixing Epon Resin 828 RS and Epicure 3115-X-70 curing agent in equal volumes. The resin and curing agent were supplied by Resolution Performance Products of Houston, TX. The solvent, 2-butanone (99%) supplied by Sigma Aldrich, was added to the mixture such that the solvent consisted of 25 vol. % of the total mixture volume. The tricomponent mixture was stirred at room temperature to obtain a homogeneous medium. The epoxy was applied onto the AA 2024-T3 panels using a draw-down bar. An effort was made to limit the exposure of the coated panels to dust by storing them in sealed containers at all times between application of the epoxy and the placement of the panels in a dust-free oven for curing. The curing stage consisted of 6 h at 60°C followed by at least 48 h at room temperature.

A glass cylinder with an O-ring insert was used as part of the electrochemical cell. The cylinder was clamped to the coated panel with the cylinder sectioning, a test area of 7.07 cm^2 of the coated panel, which was 5 × 8 in. in overall dimension. The location of the test area on a panel was done after careful inspection of the coated panel to ensure that the test area was free of defects and approximately uniform in thickness. The thickness of the test area was measured as an average of 13 thickness measurements over the test area performed using an Elcometer 345 NS, supplied by Elcometer Instruments Ltd. of Rochester Hills, MI. The outside perimeter of the cylinder was marked to identify the test area on a given panel.

The two-electrode electrochemical cell used included the substrate as the working electrode and a Pt mesh as the counter electrode. The cylinder was filed with sufficient electrolyte to cover the counter electrode that was placed approximately 5 mm from the surface of the coating. The instruments used for electrochemical measurements were a Gamry PCI4/300 potentiostat and a FAS2 Femtostat potentiostat. These instruments were controlled by the software Gamry Framework Version 4.21/EIS 300, with the instruments and software supplied by Gamry Instruments, Inc. of Willow Grove, PA. Two types of electrochemical impedance spectroscopy (EIS) experiments were conducted. One was a single frequency experiment, where the impedance response of an applied single frequency of 10 kHz was monitored every 60 s for approximately 24 h. The other was a conventional EIS experiment which consisted of measuring the response associated with applied frequencies over a 100 kHz to 0.01 Hz range with an acquisition rate of ten points per decade. For both experiments a 20 mV amplitude perturbation potential was employed.

Experiments were conducted to characterize the response of the epoxy coating to cyclic wetting and drying stages. Continuous immersion for approximately 24 h in a 0.05 M NaCl medium represented the wetting stage. Two drying stages were used: (*i*) a natural drying stage where the coated panel was placed in a dessicator with the cylinder and O-ring removed and (*ii*) a simulated RTIL drying stage where the test area was exposed to the hydrophilic RTIL 1-butyl-1-methylpyrrolidinium trifluoromethanesulfonate ($C_{10}H_{20}F_3NO_3S$). The ionic liquid was supplied by EMD Chemicals, Inc. of Gibbstown, NJ, with a purity rating in excess of 99%.

A cycle of the wetting-RTIL drying experiment was conducted by exposing the test area to the 0.05 M NaCl medium for approximately 24 h. A single frequency EIS experiment was performed during this time to monitor the changes in the coating. After the 24 h period a conventional EIS experiment was conducted. The cylinder was removed and the test area wiped with a Kimwipes tissue to remove any of the NaCl solution on the surface. A clean cylinder and O-ring were then clamped to the test area. The RTIL electrolyte was then introduced to the cylinder with a cleaned counter electrode. The test area was exposed to the RTIL for approximately 24 h during which a single frequency EIS experiment was performed to monitor the changes in the coating. Following the 24 h period, a conventional EIS experiment was conducted. The RTIL and cylinder with O-ring was removed and the test area wiped with a Kimwipes to remove residual RTIL on the surface of the coating. The test area was then ready for another cycle. The used RTIL was replaced with pristine RTIL every three cycles as to avoid using RTIL that was saturated with water.

The wetting stage of the procedure for a cycle of the wetting-natural drying experiment was as described in the preceding paragraph. The drying stage was different with the natural drying stage being performed by placing the panel, without cylinder and O-ring, in a dessicator for 24 h. The changes associated with a natural drying stage could not be monitored by single frequency EIS or by conventional EIS because of the lack of an electrochemical contact.

In addition to the cyclic experiments, continuous wetting and continuous RTIL drying experiments were conducted by immersing test areas in 0.05 M NaCl and RTIL media, respectively. These test areas were monitored by performing conventional EIS experiments every 24 h. The thickness in micrometers of the various epoxy coatings used in the experiments of cyclic wetting-RTIL drying, cyclic wetting-natural drying, continuous wetting, and continuous drying were 32 ± 4, 42 ± 5, 46 ± 8, and 64 ± 13 μm, respectively. These measurements represent the average of 13 individual measurements of the thickness of the test area.

Results and Discussion

There was little difference observed in the EIS responses of the test area under continuous immersion in NaCl from days 1 through 16. Similarly, there was little difference observed in the EIS responses of the test area under continuous immersion in RTIL from days 1 through 16. The Nyquist plots for the area under constant

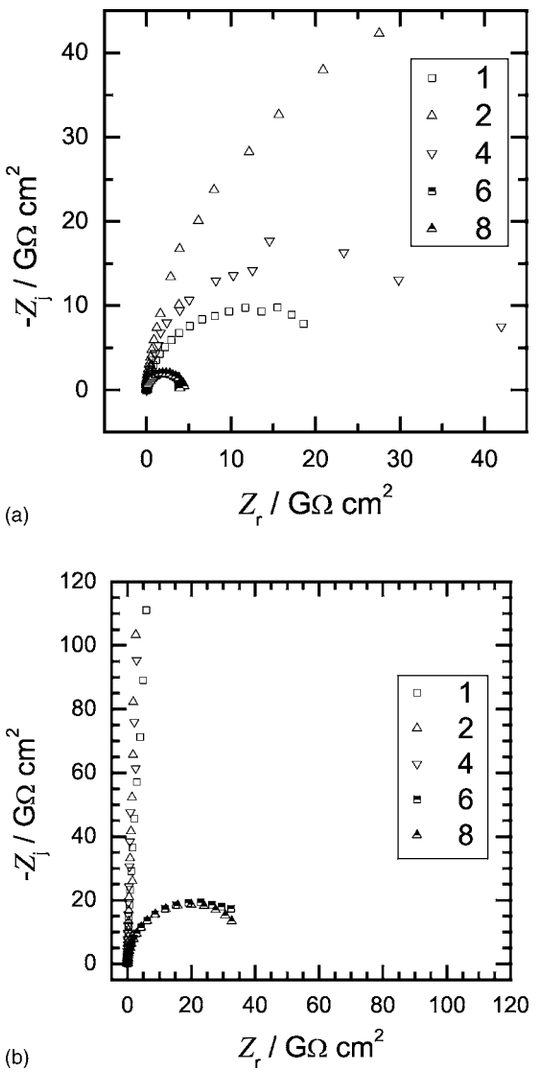

Figure 1. Impedance results for the test area exposed to the cyclic NaCl wetting-RTIL drying with cycle number as a parameter. Nyquist plots obtained after (a) 0.05 M NaCl immersion and (b) ionic liquid immersion.

NaCl immersion were similar to that of the area under NaCl immersion during cyclic immersion between 0.05 M NaCl wetting and RTIL drying that is shown in Fig. 1a. This indicated that there was a resistance component associated with the test area. The Nyquist plots associated with the area under constant RTIL immersion were similar to the drying stage of cycle 1 for the area under cyclic immersion between 0.05 M NaCl wetting and RTIL drying that is shown in Fig. 1b. This indicated that there was a capacitance response and an absence of any measurable resistance component associated with the test area under RTIL. The capacitance response of the coating for the frequency range employed demonstrated that the RTIL could be used to measure the dielectric properties of the coating. It was concluded that constant immersion in either 0.05 M NaCl or RTIL for 16 days did not alter the epoxy coating to the extent that it would manifest itself in changes to the EIS response.

The experimental results associated with the test area under cyclic, immersion between 0.05 M NaCl wetting and RTIL drying are shown in Fig. 1a and b, respectively, with cycle as a parameter. The data associated with immersion in NaCl are represented as cycles 1, 2, 3… and the data associated with immersion in RTIL are represented as cycles 1.5, 2.5, 3.5… . The Nyquist plot for the 0.05 M NaCl immersion indicated that there was a resistance component

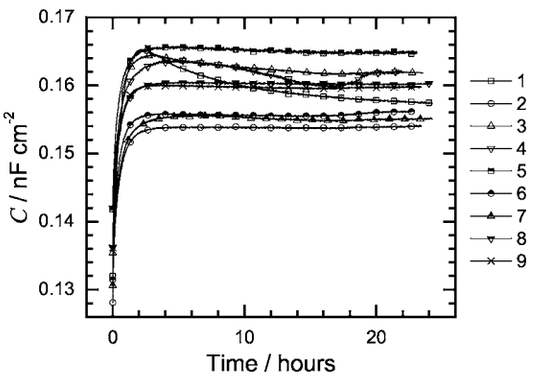

Figure 2. Capacitance evolution calculated from single frequency impedance data obtained during immersion in 0.05 M NaCl with cycle number as a parameter for the test area exposed to cyclic NaCl wetting-RTIL drying.

associated with the EIS response for any given cycle. This resistance component appeared to increase from cycles 1 to 2 and then decreased from cycles 2 to 8. The Nyquist plot for the RTIL immersion indicated that there was an absence of any observable resistance component for cycles 1 through 4. However, there was a resistance component for cycles 6 through 8.

The Nyquist plots of the experimental results associated with the test area under cyclic NaCl wetting-natural drying conditions were similar to those of the wetting stage of the test area under cyclic immersion between 0.05 M NaCl and RTIL. Two blisters, approximately 1 mm^2 each, appeared after the first cycle and this was accompanied by a decrease in the resistance component. An increase in the resistance component was observed after cycle 2 and this was attributed to the products of corrosion beneath the blisters blocking further corrosion.

The experimental results of capacitance as a function of immersion time in 0.05 M NaCl is shown in Fig. 2 for the test area exposed to cyclic NaCl wetting-RTIL drying. The value of the capacitance as a function of time $C(t)$ was calculated by relating the angular frequency ω and the imaginary part of the impedance Z_j using

$$C = (-\omega Z_j)^{-1} \quad [8]$$

for the EIS data obtained at the single frequency of 10 kHz every 60 s. The plot of $C(t)$ associated with cycle 1 included an exponential increase in C with time followed by an uncharacteristic nonlinear decrease in C with time. The trend in the value of $C(t)$ associated with cycle 2 included an exponential increase for the first 2 h after which there was a decrease followed by an increase. This increase and decrease may not be observable for cycle 2 in the scale used in Fig. 2. The trends associated with the plots of $C(t)$ for the remaining cycles of NaCl immersion were similar to that observed in cycle 2. The trend of the decrease and increase in C after the initial exponential increase in C can be seen for cycles 3, 4, and 5. This trend became less apparent with increase in cycles.

The results of capacitance as a function of immersion time in RTIL are shown in Fig. 3 for the test area exposed to cyclic NaCl wetting-RTIL drying. The trend associated with cycle 1.5 included an exponential decrease in C during the first 3 h followed by an approximately unchanged value in C with time. This trend was also associated with cycles 2.5 and 6.5–9.5 for the RTIL immersion. The trend in capacitance observed in Fig. 3 was not similar to the trends reported by Park et al. for the capacitance response of a coating system undergoing natural drying[13] as the reported trends did not include an initial exponential decrease in capacitance. The trend in C associated with cycles 3.5, 4.5, and 5.5 included an exponential decrease for the first hour followed by a clearly observable increase for the following 2–3 h, after which there was an exponential de-

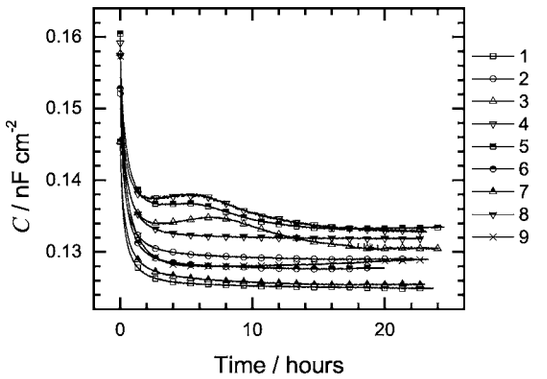

Figure 3. Capacitance evolution calculated from single frequency impedance data obtained during immersion in RTIL with cycle number as a parameter for the test area exposed to cyclic NaCl wetting-RTIL drying.

crease in C that approached an asymptotic value. This trend represented an uncharacteristic response of the capacitance and may be associated with the redistribution of water in the coating.

The results of capacitance as a function of immersion time in 0.05 M NaCl is shown in Fig. 4 for the test area exposed to cyclic NaCl wetting-natural drying. The results for cycle 1 were omitted, as there were large oscillations in the capacitance during the first hour of immersion. This capacitance response was attributed to blister formation as during this time two blisters appeared. The experiment on this test area was continued despite the blisters. The trends in the value of C associated with cycles 2–9 included an exponential increase followed by an asymptotic approach to a steady value.

The experimental results reported here were for specific test areas under various conditions. The trends observed in these results with respect to NaCl wetting, RTIL drying, and natural drying were also observed in results associated with test areas that are not reported here.

Comparison of the EIS spectra associated with the different test areas was performed using the value of the modulus of impedance at 0.01 Hz, $|Z_{0.01\ \mathrm{Hz}}|$, and the value of the capacitance calculated at 10 kHz, $C_{10\ \mathrm{kHz}}$. The values of $|Z_{0.01\ \mathrm{Hz}}|$ are shown in Fig. 5a as a function of cycle for the various experiments. The results associated with the test areas under constant immersion in 0.05 M NaCl and RTIL are given as functions of cycle although these test areas were not subjected to cyclic conditions. The daily data associated with these constant immersion experiments were converted to a cyclic

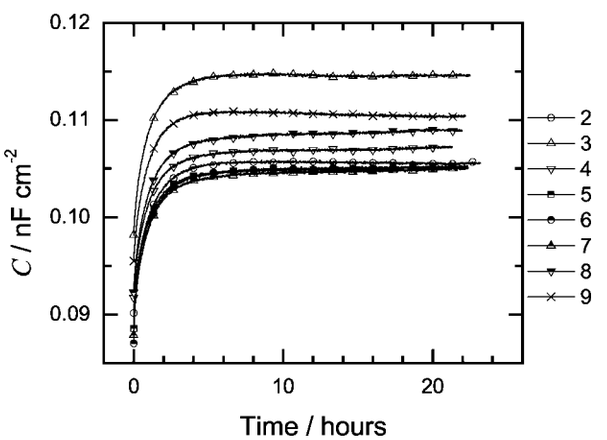

Figure 4. Capacitance evolution calculated from single frequency data obtained during immersion in 0.05 M NaCl with cycle number as a parameter for the test area exposed to cyclic NaCl wetting-natural drying.

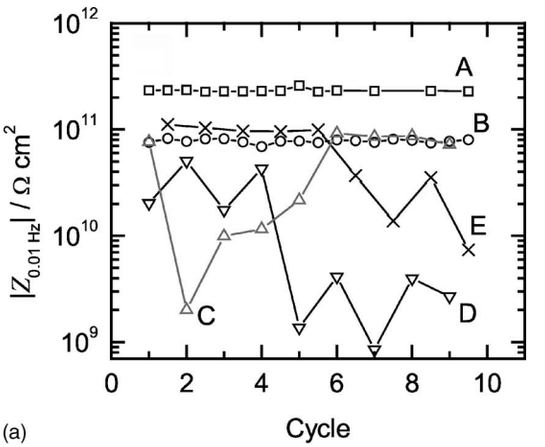

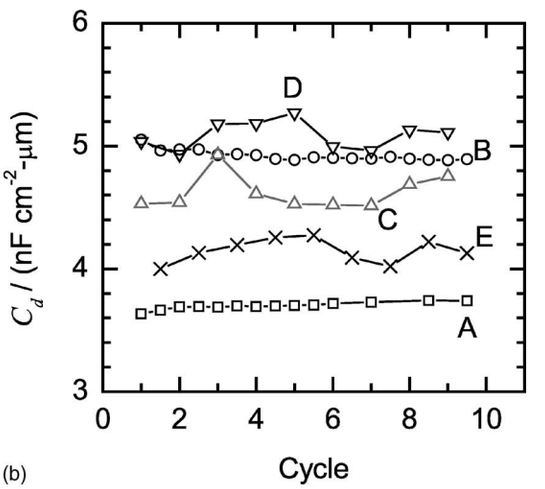

Figure 5. (a) Low-frequency modulus and (b) scaled capacitance at 10 kHz as functions of cycle number with experimental condition as a parameter. Key: A-constant immersion in RTIL; B-constant immersion in 0.05 M NaCl; C-wetting stage of cyclic NaCl wetting-natural drying; D-wetting stage of cyclic NaCl wetting-RTIL drying; E-drying stage of cyclic NaCl wetting-RTIL drying.

representation using an increment of 0.5 cycle to correspond to a 24 h period. The $|Z_{0.01\ \mathrm{Hz}}|$ value of the test areas under constant immersion in 0.05 NaCl and RTIL were approximately $10^{11}\ \Omega\ \mathrm{cm}^2$ and $2 \times 10^{11}\ \Omega\ \mathrm{cm}^2$, respectively, for cycles 1 through 9. This consistency indicated that immersion in either 0.05 M NaCl or RTIL did not degrade the epoxy coating to the extent that there were changes in the resistance barrier effect.

The $|Z_{0.01\ \mathrm{Hz}}|$ value associated with the wetting stage of the test area that was under cyclic NaCl wetting-natural drying conditions was $8 \times 10^{10}\ \Omega\ \mathrm{cm}^2$ for cycle 1, decreased to $2 \times 10^{9}\ \Omega\ \mathrm{cm}^2$ for cycle 2 and then increased to $10^{11}\ \Omega\ \mathrm{cm}^2$ by cycle 6. From cycles 6 through 8 the $|Z_{0.01\ \mathrm{Hz}}|$ values were approximately $10^{11}\ \Omega\ \mathrm{cm}^2$. The decrease and increase in the $|Z_{0.01\ \mathrm{Hz}}|$ values between cycles 1 and 6 was attributed to blisters as described before. The similarity between the $|Z_{0.01\ \mathrm{Hz}}|$ values of the test areas under constant NaCl immersion and cyclic NaCl wetting-natural drying (except for cycles 2 through 6) indicated that the latter condition did not significantly alter the epoxy coating to the extent that there was a change in the resistance barrier effect.

The $|Z_{0.01\ \mathrm{Hz}}|$ values associated with the test area under the cyclic NaCl wetting-RTIL drying indicated that there were changes in the barrier effect of the epoxy coating between cycles 1 and 8. The

$|Z_{0.01\ Hz}|$ values associated with the NaCl wetting oscillated between 2×10^{10} and $5 \times 10^{10}\ \Omega\ cm^2$ and between 9×10^8 and $4 \times 10^9\ \Omega\ cm^2$ for the first four cycles and the next five cycles, respectively. The similarity between the $|Z_{0.01\ Hz}|$ values of this test area for the first four cycles and that under constant NaCl immersion suggested that the cyclic NaCl wetting-RTIL drying conditions did not significantly influence the epoxy coating resistance property for the first four cycles. The decrease in $|Z_{0.01\ Hz}|$ for the NaCl wetting by an order of magnitude between the first four and next five cycles was significant and indicated that the NaCl wetting-RTIL drying conditions had altered the epoxy coating. Comparison of the $|Z_{0.01\ Hz}|$ values associated with the cyclic NaCl wetting-natural drying and cyclic NaCl wetting-RTIL drying conditions indicated that the use of the latter condition may be more severe to the coating's barrier property than the former.

The $|Z_{0.01\ Hz}|$ value associated with RTIL drying for the test area under cyclic NaCl wetting-RTIL drying was approximately $10^{11}\ \Omega\ cm^2$ for the first five cycles after which it decreased to a value of $7 \times 10^9\ \Omega\ cm^2$ at cycle 9. This trend supported the conclusion that the NaCl wetting-RTIL drying conditions did not alter the epoxy coating for the first four cycles after which it altered the barrier property of the epoxy coating. The decrease in the $|Z_{0.01\ Hz}|$ value associated with the drying condition was unexpected as it was assumed that the affinity for water of the RTIL would remove any water from the coating after 24 h immersion in RTIL. Two possible explanations for this observation are proposed.

Under the assumption that there are no pores in the coating and barring the ingress of the RTIL ions themselves diffusing into the epoxy, a plausible explanation for the decrease in the observed $|Z_{0.01\ Hz}|$ value would be that there is some residual electrolyte of water, Na^+, and Cl^- ions within the epoxy network that is not removed by the RTIL. This electrolyte would reduce the resistance of the coating as observed. The decrease in the $|Z_{0.01\ Hz}|$ value with cycling may then be due to the accumulation of residual electrolyte with cycling. Another plausible explanation is that there are pores in the epoxy that start from the surface and traverse towards the substrate. The entry of the ions of the RTIL into these pores would reduce the barrier afforded by the coating. The geometry of the pores may be able to accommodate the transport of the RTIL ions only after a number of cycles. These two possible explanations are reasonable, as they would predict a decrease in the $|Z_{0.01\ Hz}|$ value as observed.

The second explanation is supported by the capacitance values at approximately 24 h associated with the RTIL drying (see Fig. 3). These values were within the range of 0.125–0.134 nF cm^{-2} for the early cycles 1.5–5.5, and within the range of 0.126–0.132 nF cm^{-2} for the later cycles 6.5–9.5. The resistance component was observed in the later cycles (see Fig. 1b) and if there were trapped electrolyte within the epoxy matrix there would be corresponding increases in the capacitance for the later cycles as compared with the early cycles. This was not observed as the capacitance values for the early and late cycles were similar with the range for the early cycles encompassing the range of the later cycles.

The $C_{10\ kHz}$ values associated with the test areas under constant immersion in 0.05 M NaCl and RTIL were approximately constant at 0.106 and 0.056 $\mu F\ cm^2$ from cycles 1 through 9, respectively. The $C_{10\ kHz}$ value associated with the test area under cyclic NaCl wetting-natural drying was approximately 0.106 $\mu F\ cm^2$ from cycles 1 through 8. The $C_{10\ kHz}$ values associated with the test area under cyclic NaCl wetting and RTIL drying were 0.155 and 0.127 $\mu F\ cm^2$, respectively. Comparison of the capacitance data for test areas of different coating thickness was done under the assumption that the coating was a parallel plate capacitor. As such, the $C_{10\ kHz}$ values were scaled by the thickness of the coating using

$$C_d = C_{10\ kHz} \times L \quad [9]$$

where C_d was the scaled capacitance. The C_d values as a function of cycle are shown in Fig. 5b for the various experimental conditions.

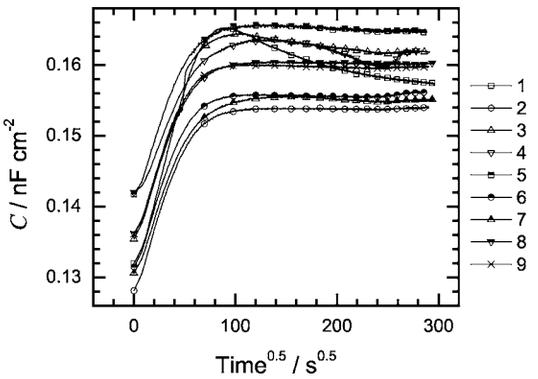

Figure 6. Capacitance calculated from single frequency impedance data obtained during immersion in 0.05 M NaCl as a function of the square root of immersion time with cycle number as a parameter for the test area exposed to cyclic NaCl wetting-RTIL drying.

The C_d values associated with the test areas under constant immersion in 0.05 M NaCl (continuous wetting) and RTIL (continuous drying) were approximately constant at 5.0 and 3.6 nF cm^2 μm, respectively, from cycles 1 through 9. These values were used to calculate the dielectric constant of the coating at 5.8 and 7.7 for the continuous drying and continuous wetting conditions. The dielectric constant of 5.8 associated with the RTIL immersion was in the range 3–8 that is reported for polymers. The C_d value associated with the wetting stages of the NaCl wetting-RTIL drying experiment was between 4.9 and 5.3 nF cm^2 μm for cycles 1–8. These C_d values agreed with the C_d value of 5.0 nF cm^2 μm associated with the continuous wetting test area. The C_d values associated with the drying stages of the NaCl wetting-RTIL drying cycles were between 4.0 and 4.4 nF cm^2 μm. These values were larger than the value of 3.6 nF cm^2 μm that was associated with the test area under continuous drying. This suggested that the coating was not completely dried during the drying stage and lends support to the proposed explanation that there was electrolyte accumulation in the coating during the cycles. The C_d values associated with the sample under cyclic NaCl wetting-natural drying conditions were approximately 4.6 nF cm^2 μm, except for cycle 3, indicating that there was little change in the capacitance with natural drying.

The characteristic capacitance evolution for an organic coating undergoing water absorption is based on the solution to Fick's second law, Eq. 1.[12] The evolution with respect to the square root of time includes a linear increase in capacitance followed by an asymptotic approach to a steady value, the steady value indicating that the coating is saturated. The solution to Fick's second law is also applicable to the desorption of water.[8] Therefore, the evolution associated with desorption of water would include a linear decrease in capacitance followed by an asymptotic approach to a steady value, the steady values indicating when there is negligible desorption of water from the coating. The experimental capacitance data $C(t)$ for the test area under cyclic NaCl wetting-RTIL drying immersion is shown for the wetting and drying stages as functions of $t^{0.5}$ in Fig. 6 and 7, respectively. The experimental data of cycle 1 included a peak in the capacitance evolution, which was uncharacteristic of a Fickian evolution. This type of anomalous evolution has been attributed to water accumulating at the interface between the coating and the metal.[11] This anomalous behavior was not seen in any of the other cycles associated with wetting. However, an anomalous peak in the capacitance response was observed in cycles 3.5, 4.5 and 5.5 that were associated with the drying stages. Another type of anomalous behavior was observed in cycle 4 where there was a drop in the capacitance followed by a rise after the capacitance had leveled off. Explanations for these anomalous behaviors are not known at the present, but it may involve the redistribution of water in the coating

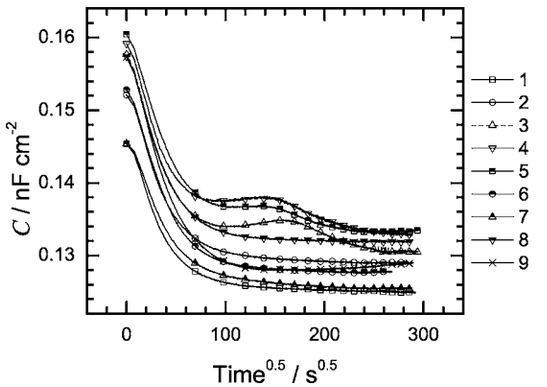

Figure 7. Capacitance calculated from single frequency impedance data obtained during immersion in RTIL as a function of the square root of immersion time with cycle number as a parameter for the test area exposed to cyclic NaCl wetting-RTIL drying.

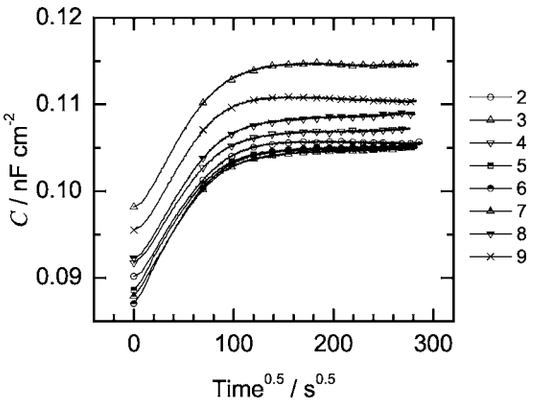

Figure 8. Capacitance calculated from single frequency impedance data obtained during immersion in 0.05 M NaCl as a function of the square root of immersion time with cycle number as a parameter for the test area exposed to cyclic NaCl wetting-natural drying.

and accumulation of water at the coating/metal interface. Apart from the anomalous behavior associated with cycles 1, 4, 3.5, 4.5, and 5.5, the general trend observed was that the capacitance evolution was more in agreement with a Fickian-type evolution as the cycles increased. This would indicate that the coating medium was becoming more homogeneous. Features associated with an inhomogeneous coating include voids and densely packed regions. The cyclic wetting and RTIL drying conditions probably facilitated plasticization such that these features were reduced.

The experimental capacitance data $C(t)$ for the test area under cyclic NaCl wetting-natural drying conditions is shown for the wetting stages as functions of $t^{0.5}$ in Fig. 8. The capacitance evolution of this test area was consistent with a Fickian-type evolution for cycles 2–9. The capacitance values associated with the saturated coating after 24 h were within the range of 0.105–0.115 nF cm^{-2}. This was a different range as compared to the range of saturated capacitance values associated with the wetting stages of the test area under cyclic NaCl wetting-RTIL drying which was between 0.154 and 0.165 nF cm^{-2} (see Fig. 6). The difference in ranges was attributed to the different thickness in test areas. The differences between the maximum and minimum values of the ranges were 0.010 and 0.011 nF cm^{-2} for the test areas under cyclic NaCl wetting-natural drying and cyclic NaCl wetting-RTIL drying conditions, respectively. The similarity between these differences supported the simulation of the drying condition by the RTIL.

The values of the diffusion coefficients associated with wetting and drying obtained from the short-time model of Eq. 7 are represented by $D_{\text{in},s}$ and $D_{\text{out},s}$, respectively. The C_o and C_s parameters used for the calculation of $D_{\text{in},s}$ and $D_{\text{out},s}$ are listed in Table I together with the calculated values of $D_{\text{in},s}$ and $D_{\text{out},s}$ for the cycles. The $D_{\text{in},s}$ and $D_{\text{out},s}$ values associated with the cyclic 0.05 M NaCl wetting-RTIL drying are shown as functions of cycle in Fig. 9a. The slope over the first 2500 s associated with cycle 1, wetting in NaCl, shown in Fig. 6 was larger than any of the other slopes and the corresponding value of $D_{\text{in},s}$, 4.0×10^{-13} m^2 s^{-1}, was larger than the other diffusion coefficients. This suggested that the phenomena which contributed to the peak behavior associated with the cycle 1 influenced the calculated $D_{\text{in},s}$ value significantly. The $D_{\text{in},s}$ and $D_{\text{out},s}$ values for the wetting and drying stages ranged from 2.93 to 3.35×10^{-13} m^2 s^{-1} for wetting (excluding cycle 1) and $2.05–3.10 \times 10^{-13}$ m^2 s^{-1} for drying. The trend of the data presented in Fig. 9a suggests that there may be a difference between the values of $D_{\text{in},s}$ and $D_{\text{out},s}$. This trend is supported by the difference in the average values where the average $D_{\text{in},s}$ value was $3.1 \pm 0.2 \times 10^{-13}$ m^2 s^{-1} and the average $D_{\text{out},s}$ value was $2.6 \pm 0.3 \times 10^{-13}$ m^2 s^{-1}.

The capacitance data $C(t)$ were also analyzed by the regression of the data to a series expansion of the Fickian solution given in Eq. 6. The values of the diffusion coefficient associated with wetting and

Table I. Parameter values used for the calculation of the short-time model diffusion coefficients associated with the cyclic NaCl wetting-RTIL drying experiment.

Stage	Cycle	C_0 (nF cm^{-2})	C_s (nF cm^{-2})	$D_{\text{in},s} \times 10^{13}$ (m^2 s^{-1})	$D_{\text{out},s}$ (m^2 s^{-1})
Wetting	1	0.132	0.157	4.00	
Drying	1.5	0.145	0.125		3.07
Wetting	2	0.128	0.154	2.93	
Drying	2.5	0.152	0.129		3.10
Wetting	3	0.135	0.162	3.25	
Drying	3.5	0.158	0.130		2.56
Wetting	4	0.142	0.162	3.17	
Drying	4.5	0.159	0.133		2.60
Wetting	5	0.142	0.165	3.27	
Drying	5.5	0.160	0.133		2.05
Wetting	6	0.131	0.156	3.35	
Drying	6.5	0.153	0.128		2.35
Wetting	7	0.131	0.155	2.93	
Drying	7.5	0.145	0.125		2.53
Wetting	8	0.136	0.160	3.09	
Drying	8.5	0.157	0.132		2.60

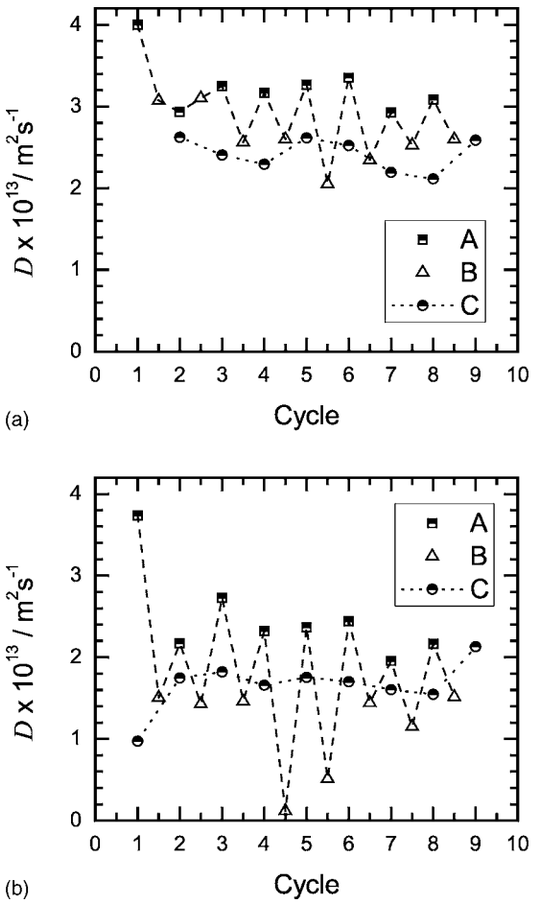

Figure 9. Diffusion coefficient parameter D calculated using (a) the short time model and (b) the series solution model as a function of cycle number with experimental condition as a parameter. Key: A-D_{in} for the wetting stage of the cyclic NaCl wetting-RTIL drying experiment; B-D_{out} for the drying stage of the cyclic NaCl wetting-RTIL drying experiment; C-D_{in} for the wetting stage of the cyclic NaCl wetting-natural drying experiment.

drying obtained from the regression are represented by $D_{in,fit}$ and $D_{out,fit}$, respectively. A nonlinear least squares regression algorithm was used to perform the regression of the $C(t)$ data to Eq. 6 to yield the four parameters C_o, C_s, $D_{in,fit}$ and $D_{out,fit}$. The values of C_o, C_s, $D_{in,fit}$ and $D_{out,fit}$ are listed in Table II. Also listed is the value of the fit parameter R^2. The $D_{in,fit}$ and $D_{out,fit}$ values are shown as functions of the cycle in Fig. 9b. The $D_{in,fit}$ value associated with the regression for cycle 1 was 3.74×10^{-13} m^2 s^{-1} with the corresponding R^2 parameter of 0.51 indicating that there was not a good fit of the model to the experimental data. The fit to cycle's 4.5 and 5.5 data did not agree with the data by visual examination although the R^2 parameters were 0.81 and 0.84, respectively. The corresponding values of $D_{out,fit}$ were 0.11×10^{-13} m^2 s^{-1} and 0.51×10^{-13} m^2 s^{-1}, respectively. Excluding the $D_{in,fit}$ value associated with cycle 1 and the $D_{out,fit}$ values associated with cycles 4.5 and 5.5, the $D_{in,fit}$ values ranged from 2.17 to 2.73×10^{-13} m^2 s^{-1} and the $D_{out,fit}$ values ranged from 1.15 to 1.52×10^{-13} m^2 s^{-1}. The average values for $D_{in,fit}$ and $D_{out,fit}$ were $2.3 \pm 0.3 \times 10^{-13}$ m^2 s^{-1} and $1.4 \pm 0.1 \times 10^{-13}$ m^2 s^{-1}, respectively. These average values supported the observed trend of the data where the diffusion coefficient for wetting $D_{in,fit}$ was larger than the diffusion coefficient for drying $D_{out,fit}$.

Included in Fig. 9a and b are the values of $D_{in,s}$ and $D_{in,fit}$ associated with the cyclic NaCl wetting-natural drying test area. These values and the values of the C_o and C_s parameters used in the calculation of $D_{in,s}$ and $D_{in,fit}$ are listed in Tables III and IV. The values of $D_{in,s}$ were calculated using the short-time model of Eq. 7 and $D_{in,fit}$ values were calculated by the regression of the $C(t)$ data to Eq. 6. The trend where the value of $D_{in,s}$ for this test area was less than the value of $D_{in,s}$ and $D_{out,s}$ for the test area exposed to cyclic NaCl wetting-RTIL drying was observed in Fig. 9a. The average value of $D_{in,s}$ associated with the cyclic NaCl wetting-natural drying test area was $2.4 \pm 0.2 \times 10^{-13}$ m^2 s^{-1}, lower than the averages of $D_{in,s}$ and $D_{out,s}$ associated with the test area exposed to cyclic NaCl wetting-RTIL drying. The trend where the value of $D_{in,fit}$ for the test area exposed to cyclic NaCl wetting-natural drying was less than the value of $D_{in,fit}$ and greater than $D_{out,fit}$ for the test area exposed to cyclic NaCl wetting-RTIL drying was observed in Fig. 9b. This trend was supported by the average value of $D_{in,fit}$ associated with the cyclic NaCl wetting-natural drying test area which was $1.7 \pm 0.2 \times 10^{-13}$ m^2 s^{-1}.

The average values for $D_{in,s}$ and $D_{in,fit}$ are shown in Fig. 10 with an error of one standard deviation. The values associated with water absorption were in good agreement with reported values for epoxy systems.[4] It can be clearly seen that the average values of water ingress $D_{in,s}$ and $D_{in,fit}$ associated with the cyclic NaCl wetting-RTIL

Table II. Parameter values used for the calculation of the series solution model diffusion coefficients associated with the cyclic NaCl wetting-RTIL drying experiment.

Stage	Cycle	C_0 (nF cm^{-2})	C_s (nF cm^{-2})	$D_{in,fit} \times 10^{13}$ (m^2 s^{-1})	$D_{out,fit} \times 10^{13}$ (m^2 s^{-1})	R^2
Wetting	1	0.127	0.160	3.74		0.509
Drying	1.5	0.143	0.125		1.50	0.966
Wetting	2	0.129	0.154	2.17		0.996
Drying	2.5	0.150	0.129		1.43	0.971
Wetting	3	0.133	0.162	2.73		0.885
Drying	3.5	0.154	0.132		1.46	0.731
Wetting	4	0.140	0.162	2.32		0.831
Drying	4.5	0.143	0.132		0.118	0.808
Wetting	5	0.141	0.165	2.37		0.980
Drying	5.5	0.150	0.134		0.511	0.836
Wetting	6	0.132	0.156	2.44		0.991
Drying	6.5	0.151	0.128		1.44	0.984
Wetting	7	0.131	0.155	1.95		0.987
Drying	7.5	0.143	0.126		1.15	0.958
Wetting	8	0.136	0.160	2.17		0.997
Drying	8.5	0.155	0.132		1.52	0.984

Table III. Parameter values used for the calculation of the short-time model diffusion coefficients associated with the cyclic NaCl wetting-natural drying experiment.

Stage	Cycle	C_0 (nF cm^{-2})	C_s (nF cm^{-2})	$D_{in,s} \times 10^{13}$ (m^2 s^{-1})
Wetting	1			
Wetting	2	0.090	0.106	2.62
Wetting	3	0.098	0.115	2.41
Wetting	4	0.092	0.107	2.29
Wetting	5	0.089	0.105	2.62
Wetting	6	0.087	0.105	2.52
Wetting	7	0.088	0.105	2.19
Wetting	8	0.092	0.109	2.11
Wetting	9	0.096	0.110	2.59

drying experiment were larger than the $D_{out,s}$ and $D_{out,fit}$, respectively. However, it was observed that the difference between $D_{in,fit}$ and $D_{out,fit}$ was significant while that between $D_{in,s}$ and $D_{out,s}$ was not. This observation was attributed to the calculation method used. The series model, Eq. 6, employed the full set of data as compared to the short-time model, Eq. 7, which was based on the slope of $C(t^{0.5})$ at short times.

The capacitance based on the fit of the series model to the data and the measured capacitance data associated with cycle 2 are shown in Fig. 11a. The evolution of the capacitance for the short-time model is also shown in Fig. 11a and was calculated using the $D_{in,s}$, C_0, and C_s parameters associated with the short-time model of cycle 2 and inserted into the series solution of Eq. 6. The series model capacitance and the measured capacitance were in agreement for the time period considered. The short-time capacitance agreed well with the measured capacitance for the period less than 900 s and the period greater than 22,500 s. These periods represented time frames where the capacitance change with $t^{0.5}$ was either linear or negligible. For the time period greater than 900 s and less than 22,500 s the capacitance change with $t^{0.5}$ was nonlinear. In Fig. 11b, the measured, series model and short-time model capacitance are shown as functions of $t^{0.5}$ for cycle 2.5, a cycle associated with the drying stage of the test area exposed to cyclic NaCl wetting-RTIL drying conditions. Agreement between the series model and measured capacitance was observed while there was inconsistency between the short-time model and measured capacitance. The influence of the model used in calculating D_{in} was also observed for the cyclic NaCl wetting–natural drying results.

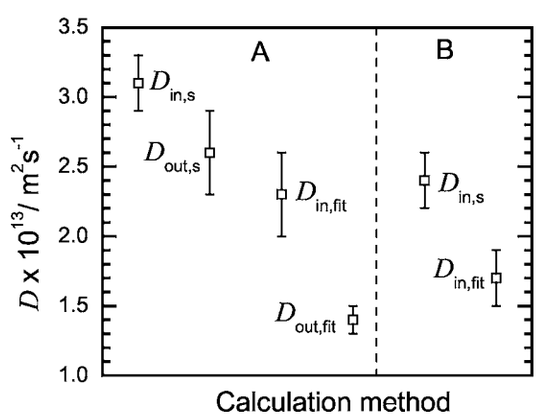

Figure 10. Average values of D_{in} and D_{out} with associated errors of one standard deviation obtained using the short-time approximate model and series solution model. Key: A-cyclic NaCl wetting-RTIL drying experiment and B-cyclic NaCl wetting-natural drying experiment.

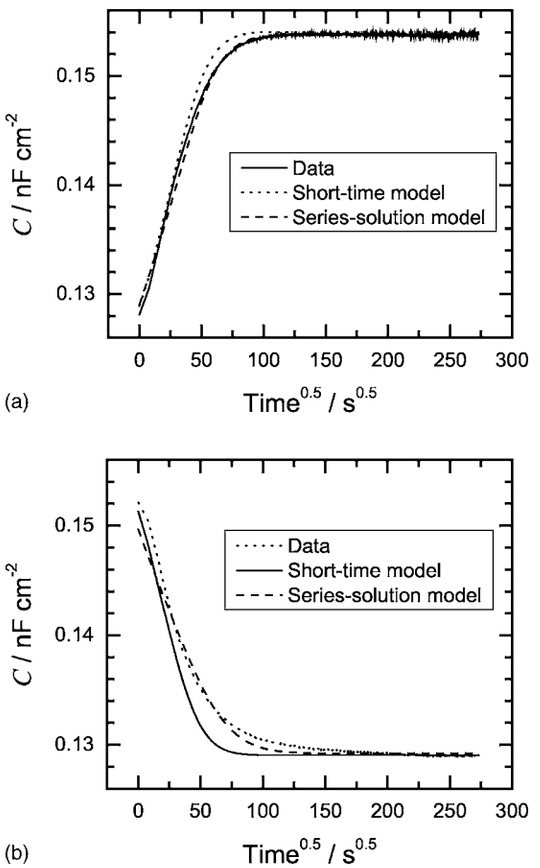

Figure 11. Capacitance calculated from single frequency data as a function of the square root of immersion time associated with the test area exposed to cyclic NaCl wetting-RTIL drying conditions. (a) Cycle 2 (wetting stage) and (b) cycle 2.5 (drying stage). Included in the figures are the capacitance evolution based on the short-time model and series model parameters.

The difference between $D_{in,fit}$ and $D_{out,fit}$ for the cyclic NaCl wetting-RTIL drying experiment demonstrated that the ingress of water for a given test area was faster than the egress. For coatings where D_{in} is significantly different from D_{out}, wet-dry cycling would become influential with respect to water accumulation and it is for such coatings that the knowledge of D_{in} and D_{out} would be important.

Conclusions

The measurement of the diffusion coefficient associated with the absorption of water by gravimetry and capacitance methods has

Table IV. Parameter values used for the calculation of the series model diffusion coefficients associated with the cyclic NaCl wetting-natural drying experiment.

Stage	Cycle	C_0 (nF cm^{-2})	C_s (nF cm^{-2})	$D_{in,fit} \times 10^{13}$ (m^2 s^{-1})
Wetting	1	0.212	0.254	0.97
Wetting	2	0.090	0.106	1.75
Wetting	3	0.097	0.114	1.82
Wetting	4	0.092	0.107	1.66
Wetting	5	0.090	0.105	1.75
Wetting	6	0.088	0.105	1.70
Wetting	7	0.089	0.105	1.60
Wetting	8	0.092	0.109	1.55
Wetting	9	0.094	0.110	2.13

been well established in literature. The measurement of the diffusion coefficient associated with the desorption of water has been heretofore limited to the gravimetric method. The recent work reported[14] and the work presented in this effort have introduced the methodology whereby RTILs in conjunction with the capacitance method can be used to determine the diffusion coefficient associated with the desorption of water from coating films.

The results presented for the epoxy coating demonstrated a trend where the average value of D_{in} was slightly larger than the average value of D_{out} for the number of cycles considered irrespective of the model used for the diffusion coefficient calculation. The absence of a resistance component in the spectra associated with the early cycles of the drying stage of the test area undergoing cyclic NaCl wetting-RTIL drying was attributed to the RTIL removing the water that had diffused into the coating during the wetting stage. During the later cycles, a resistance component appeared that was attributed to the entry of RTIL into the coating thereby introducing a resistance effect or/and the accumulation of electrolyte within the matrix of the coating.

The capacitance evolution associated with the NaCl wetting-RTIL drying test area was more in agreement with a Fickian-type evolution as the number of cycles increased. This indicated that the coating medium was becoming more homogeneous, probably due to plasticization facilitated by the wet-RTIL dry conditions. The capacitance evolution associated with the drying stage was also consistent with a Fickian-type evolution, which demonstrated the usefulness of RTIL as a nonaqueous media for desorption studies.

Acknowledgments

The Army Research Laboratory and the Air Force Office of Scientific Research supported this work under contract no. W911NF-04-2-0029 and grant no. FA9550-04-1-0368, respectively.

North Dakota State University assisted in meeting the publication costs of this article.

List of Symbols

c	concentration of water (mol cm^{-3})
C	capacitance (F cm^{-2})
C_t	capacitance at time t (F cm^{-2})
C_s	capacitance at saturated condition (F cm^{-2})
C_t	capacitance at initial time $t = 0$ (F cm^{-2})
$C_{10\ kHz}$	capacitance calculated from impedance data at frequency 10 kHz (F cm^{-2})
C_d	capacitance scaled by coating thickness (F cm^{-1})
D	diffusion coefficient of water (cm^2 s^{-1})
D_{in}	diffusion coefficient of the ingress of water (cm^2 s^{-1})
D_{out}	diffusion coefficient of the egress of water (cm^2 s^{-1})
$D_{in,s}$	diffusion coefficient of the ingress of water calculated from the short-time model (cm^2 s^{-1})
$D_{out,s}$	diffusion coefficient of the egress of water calculated from the short-time model (cm^2 s^{-1})
$D_{in,fit}$	diffusion coefficient of the ingress of water calculated from the series-solution model (cm^2 s^{-1})
$D_{out,fit}$	diffusion coefficient of the egress of water calculated from the series-solution model (cm^2 s^{-1})
L	coating thickness (cm)
M_t	mass of water absorbed by coating at time t (g)
M_s	mass of water absorbed by coating at saturation (g)
t	time (s)
Z_j	imaginary component of impedance (Ω cm^2)
Z_r	real component of impedance (Ω-cm^2)
$\lvert Z_{0.01\ Hz}\rvert$	modulus of impedance calculated at 0.01 Hz (Ω-cm^2)

Greek

ε_{H_2O}	permittivity of water (F/cm)
ϕ_t	volume fraction occupied by water at time t
ϕ_s	volume fraction occupied by water at saturation
ω	frequency (radians/s)

References

1. D. M. Brasher and A. H. Kingsbury, *J. Appl. Chem.*, **4**, 62 (1954).
2. S. A. Lindqvist, *Corrosion (Houston)*, **41**, 69 (1985).
3. F. Bellucci and L. Nicodemo, *Corrosion (Houston)*, **49**, 235 (1993).
4. E. P. M. Van Westing, G. M. Ferrari, and J. H. W. De Wit, *Corros. Sci.*, **36**, 957 (1994).
5. V. B. Miskovic-Stankovic, D. M. Drazic, and Z. Kacarevic-Popovic, *Corros. Sci.*, **38**, 1513 (1996).
6. V. B. Miskovic-Stankovic, M. D. Maksimovic, Z. Kacarevic-Popovic, and J. B. Zotovic, *Prog. Org. Coat.*, **33**, 68 (1998).
7. A. S. Castela and A. M. Simoes, *Corros. Sci.*, **45**, 1631 (2003).
8. J. Crank, *The Mathematics of Diffusion*, p. 47, Oxford University Press, New York (1989).
9. G. W. Walter, *Corros. Sci.*, **32**, 1059 (1991).
10. B. N. Popov, M. A. Alwohaibi, and R. E. White, *J. Electrochem. Soc.*, **140**, 947 (1993).
11. C. Perez, A. Collazo, M. Izquierdo, P. Merino, and X. R. Novoa, *Prog. Org. Coat.*, **36**, 102 (1999).
12. F. Deflorian, L. Fedrizzi, S. Rossi, and P. L. Bonora, *Electrochim. Acta*, **44**, 4243 (1999).
13. J. H. Park, G. D. Lee, H. Ooshige, A. Nishikata, and T. Tsuru, *Corros. Sci.*, **45**, 1881 (2003).
14. A. M. Simoes, D. Tallman, and G. P. Bierwagen, *Electrochem. Solid-State Lett.*, **8**, 60 (2005).
15. M. M. Wind and H. J. W. Lenderink, *Prog. Org. Coat.*, **28**, 239 (1996).
16. H. Ohno, M. Yoshizawa, and T. Mizumo, *Electrochemical Aspects of Ionic Liquids*, p. 75, Wiley, Hoboken, NJ (2005).
17. A. Berthod and S. Carda-Broch, *Actualite Chimique*, **271**, 24 (2004).
18. M. F. Arenas and R. G. Reddy, *J. Min. Met.*, **39**, 81 (2003).